



Received: 6 December 2018 | Revised: 3 April 2019 | Accepted: 8 April 2019

DOI: 10.1111/cas.14020

ORIGINAL ARTICLE

Cancer Science WILEY

Epidermal growth factor receptor-targeted molecular imaging of colorectal tumors: Detection and treatment evaluation of tumors in animal models

Yoshihiko Miyamoto¹  | Naoki Muguruma¹ | Shota Fujimoto¹ | Yasuyuki Okada¹ | Yoshifumi Kida¹ | Fumika Nakamura¹ | Kumiko Tanaka¹ | Tadahiko Nakagawa² | Shinji Kitamura¹ | Koichi Okamoto¹ | Hiroshi Miyamoto¹ | Yasushi Sato³ | Tetsuji Takayama¹ 

¹Department of Gastroenterology and Oncology, University of Tokushima Faculty of Medicine Graduate School of Medical Sciences, Tokushima, Japan

²Department of Health and Nutrition, University of Shimane Faculty of Nursing, Izumo, Japan

³Department of Community Medicine for Gastroenterology and Oncology, Tokushima University Graduate School, Tokushima, Japan

Correspondence

Tetsuji Takayama, Department of Gastroenterology and Oncology, Institute of Biomedical Sciences, Tokushima University Graduate School, Tokushima, Japan.
Email: takayama@tokushima-u.ac.jp

Funding information

This study was partly supported by JSPS KAKENHI Grant Number 25461034 and JFE (The Japanese Foundation for Research and Promotion of Endoscopy) Grant.

Abstract

To overcome the problem of overlooking colorectal tumors, a new and highly sensitive modality of colonoscopy is needed. Moreover, it is also important to establish a new modality to evaluate viable tumor volume in primary lesions of colorectal cancer (CRC) during chemotherapy. Therefore, we carried out molecular imaging of colorectal tumors targeting epidermal growth factor receptor (EGFR), which is highly expressed on tumor cells, for evaluating chemotherapeutic efficacy and for endoscopic detection of colorectal adenomas. We first attempted to image five CRC cell lines with various levels of EGFR expression using an Alexa Fluor-labeled anti-EGFR monoclonal antibody (AF-EGFR-Ab). A strong fluorescence signal was observed in the cells depending on the level of EGFR expression. When nude mice xenografted with LIM1215 CRC cells, which highly express EGFR, were i.v. injected with AF-EGFR-Ab, a strong fluorescence signal appeared in the tumor with a high signal to noise ratio, peaking at 48 hours after injection and then gradually decreasing, as shown using an IVIS Spectrum system. When the xenografted mice were treated with 5-fluorouracil, fluorescence intensity in the tumor decreased in proportion to the viable tumor cell volume. Moreover, when the colorectum of azoxymethane-treated rats was observed using a thin fluorescent endoscope with AF-EGFR-Ab, all 10 small colorectal adenomas (≤ 3 mm) were detected with a clear fluorescence signal. These preliminary results of animal experiments suggest that EGFR-targeted fluorescent molecular imaging may be useful for quantitatively evaluating cell viability in CRC during chemotherapy, and also for detecting small adenomas using a fluorescent endoscope.

Abbreviations: AF-EGFR-Ab, Alexa Fluor-labeled anti-EGFR monoclonal antibody; AOM, azoxymethane; CEA, carcinoembryonic antigen; CRC, colorectal cancer; CT, computed tomography; EGFR, epidermal growth factor receptor; S/N, signal to noise.

This is an open access article under the terms of the Creative Commons Attribution-NonCommercial License, which permits use, distribution and reproduction in any medium, provided the original work is properly cited and is not used for commercial purposes.

© 2019 The Authors. *Cancer Science* published by John Wiley & Sons Australia, Ltd on behalf of Japanese Cancer Association.

KEYWORDS

colorectal cancer, epidermal growth factor receptor, fluorescence endoscopy, molecular imaging, therapeutic efficacy

1 | INTRODUCTION

Colorectal cancer is one of the leading causes of cancer-related death worldwide.¹ It is well known that CRC develops mainly from colorectal adenoma, a precancerous lesion in the colorectum.²⁻⁴ Therefore, it is important to remove colorectal adenoma before it develops into cancer. However, it has been reported that 15%-32% of colorectal tumors are overlooked during colonoscopy.⁵ Thus, improved endoscopy capable of more sensitive detection of colorectal tumors is needed.

In addition, evaluation of tumor size in response to chemotherapy is critical in the treatment of metastatic CRC.⁶ Currently, response to treatment in CRC is evaluated by CT using RECIST criteria.⁷ Only measurable metastatic lesions in patients with CRC are evaluated by measuring tumor size in CT images based on RECIST criteria. However, it is difficult to evaluate viable tumor cells accurately because the central part of the tumor often undergoes necrosis as a result of chemotherapy or other factors.⁸⁻¹⁰ Moreover, there is no method to objectively evaluate tumor volume of primary lesions in the colorectum during chemotherapy. A new imaging modality to accurately assess viable tumor volume of CRC is therefore needed.

Molecular imaging is a good candidate modality for the detection of small colorectal tumors with high sensitivity and accurately evaluates the viability of colorectal tumors. Furthermore, molecular imaging also makes it possible to distinguish malignant and benign lesions, and to accurately assess tumor margin.¹¹ However, a practical molecular imaging technology that improves the detection of small tumors and enables evaluation of viable tumor cell volume before and after chemotherapy has yet to be established.¹²

Epidermal growth factor receptor is a transmembrane-type tyrosine kinase. EGFR is commonly expressed on the cell surface of CRC and precancerous adenomas, and is strongly associated with proliferation, invasion, metastasis, poor prognosis, and early recurrence of CRC.¹³⁻¹⁶ EGFR is expressed on the cell membrane surface, and the expression level is highest in cancer, moderate in adenoma, and very low in normal epithelia. Thus, EGFR is suitable as a target for molecular imaging of colorectal tumors.

Although several studies on molecular imaging of CRC targeting EGFR have been published,¹⁷⁻²¹ no studies on molecular imaging for precancerous adenomas targeting EGFR have been reported. In addition, no studies have investigated the utility of EGFR-targeted molecular imaging of viable tumor cells in CRC before and after treatment with anticancer agents. In the present study, we first examined whether fluorescence-labeled anti-EGFR antibody is able to visualize CRC *in vitro* and *in vivo* depending on EGFR expression level. We also investigated the utility of EGFR-targeted molecular imaging for the evaluation of viable cell volume before and after chemotherapy

in animal models of CRC. We then carried out molecular imaging of small colorectal adenomas in a rat model using a fluorescence-labeled anti-EGFR antibody.

2 | MATERIALS AND METHODS

2.1 | Cell lines

The CRC cell lines DLD-1, COLO320DM, HT-29, LIM1215, and M7609 were used. DLD-1 and COLO320DM cell lines were obtained from Health Science Research Resources Bank. HT-29 and LIM1215 cell lines were purchased from ATCC and European Collection of Cell Cultures, respectively. The M7609 cell line was kindly provided by Dr R. Machida (Hirosaki University). COLO320DM cells were maintained in DMEM supplemented with 10% FBS, 50 U/mL penicillin, and 50 U/mL streptomycin. HT-29 cells were maintained in McCoy's 5a medium supplemented with 10% FBS. The other cell lines were cultured in RPMI-1640 medium supplemented with 10% FBS, 50 U/mL penicillin, and 50 U/mL streptomycin. All cells were cultured at 37°C with 5% CO₂.

2.2 | Quantification of cell surface EGFR by flow cytometry

Quantitative flow cytometric analysis of EGFR on the cell surface was carried out using mouse antihuman EGFR monoclonal antibody (sc-120; Santa Cruz Biotechnology, Dallas, TX, USA) and Dako QIFIKIT (Dako, Glostrup, Denmark), as described previously.²² In brief, cells were incubated with a mouse antihuman EGFR monoclonal antibody. After washing the cells with PBS, they were incubated with an FITC-conjugated F(ab')₂ fragment of goat antimouse IgG polyclonal antibody in the dark. Then, the fluorescence intensity of the cells was determined by flow cytometry (Becton Dickinson, Franklin Lakes, NJ, USA). Standard beads in Dako QIFIKIT coated with a known amount of mouse IgG molecules were incubated with the FITC-conjugated F(ab')₂ fragment of goat antimouse IgG polyclonal antibody. Number of antibody binding sites per cell was calculated by comparing mean fluorescence intensity value of the cells with a calibration curve obtained by regression analysis of the mean fluorescence intensity values of the standard beads.

2.3 | *In vitro* cell imaging and fluorescence intensity

For *in vitro* cell imaging, 1×10^5 CRC cells were cultured in 35-mm dishes, and then fixed with 4% paraformaldehyde and blocked with 10% goat serum. The cells were incubated with Alexa Fluor

488-labeled mouse antihuman EGFR monoclonal antibody (AF488-EGFR-Ab; sc-120, Santa Cruz Biotechnology) at 4°C overnight. Alexa Fluor 488-labeled normal mouse IgG2a (sc-3891; Santa Cruz Biotechnology) was used as a negative control. After washing with PBS, the samples were mounted with ProLong Gold Antifade Reagent with DAPI (Thermo Fisher Scientific, Waltham, MA, USA). The cells were observed by confocal laser microscopy (Nikon A1; Nikon, Tokyo, Japan) and bench top fluorescence microscopy (BIOREVO BZ9000; Keyence, Osaka, Japan). Images were captured using the Nikon A1, and signal intensity was calculated using the intrinsic software equipped with BIOREVO in each cell.

2.4 | In vivo molecular imaging of xenograft tumors in mice

LIM1215 or COLO320DM cells (1×10^7) were inoculated into the flank of five 6-week-old female BALB/c nu/nu mice (CLEA Japan Inc. Tokyo, Japan), respectively. When the tumor reached 10 mm in diameter, 50 μ g Alexa Fluor 647-labeled mouse antihuman EGFR monoclonal antibody (AF647-EGFR-Ab, sc-120 AF647; Santa Cruz Biotechnology) was injected into the tail vein of the mice under anesthesia. Alexa Fluor 647-labeled normal IgG2a (sc-24637 AF647; Santa Cruz Biotechnology) was used as a negative control. Subsequently, fluorescent images of the xenograft tumor were observed using an IVIS Spectrum (Perkin Elmer, Waltham, MA, USA) with a 640-nm excitation filter and a 680-nm emission filter, and recorded before injection (0 minute), and at 24, 48, 72, and 96 hours after injection. To quantify fluorescence intensity, regions of interest (ROI) with a diameter of 8 mm were selected in the tumor and in the background skin of the opposite side of each mouse, and the fluorescence intensities were calculated using software as described previously.²³ All animal experiments were carried out according to the Guidelines for Animal Experiments at Tokushima University.

2.5 | Treatment with fluorouracil for xenograft tumors in nude mice

Sixteen nude mice xenografted with LIM1215 cells were randomly assigned to treatment with fluorouracil (5-FU) or a control group treated with vehicle alone ($n = 8$ per group). When the tumor size reached 3–8 mm in diameter, mice were injected with 5-FU i.p. three times (once a week for 3 weeks) at a dose of 150 mg/kg or vehicle alone according to the schedule described in Figure S1a. Tumor size was measured with a Vernier caliper to measure length and width just before giving 5-FU and just before fluorescent imaging at 3 weeks after the start of dosing. Tumor volume (V) was calculated by the modified ellipsoidal formula: $V = \text{length} \times (\text{width})^2 \times 0.5$.^{24,25} Before giving 5-FU and at 3 weeks, mice received an injection of AF647-EGFR-Ab into the tail vein and fluorescence intensity was analyzed 48 hours after injection using IVIS Spectrum. Fluorescence intensity of each tumor was calculated as described above.

2.6 | Veterinary endoscope for AOM-treated rats

Azoxymethane (AOM; Sigma-Aldrich Co., St Louis, MO, USA) was given to 10 5-week-old male F344 rats (Charles River Laboratories Japan, Inc., Yokohama, Japan) s.c. at a dose of 15 mg/kg once a week for 3 weeks according to the schedule described in Figure S1b. A Thin Endoscope for Small Animal and Laboratory Animals (TESALA) system (AVS Co., Ltd., Tokyo, Japan) was used to observe colorectal mucosa under white light. For fluorescence observation, the TESALA system equipped with a blue (excitation) filter which transmits 410–500 nm rays for excitation of the probe (WRATTEN Gelatin Filter No.47, blue; Eastman Kodak Co., Rochester, NY, USA) and a yellow (barrier) filter which transmits 510-nm rays for emission of the probe (WRATTEN Gelatin Filter No.12, yellow; Eastman Kodak Co.) was used.

At 26 weeks, rats were fasted for 24 hours and given an enema with 2 mL PBS twice prior to colonoscopy for removal of feces. During the procedure, rats were anesthetized with 2% isoflurane. A thin endoscope with a diameter of 2.7 mm (70 mm length, AE-E27110; AVS Co. Ltd) was introduced through the anus and inserted into the splenic flexure with gentle insufflation using a specially designed cannula (AE-E27110-CAN-S; AVS Co. Ltd) attached to an air-pumping unit. The scope was then slowly withdrawn and the colorectal mucosa was carefully observed under white light. A 3-mL enema with AF488-EGFR-Ab (20 μ g/mL), which was sufficient to immerse the distal side of the colorectum, was given after pretreatment with or without non-labeled mouse anti-human EGFR monoclonal antibody (200 μ g/mL, sc-120; Santa Cruz Biotechnology). After 3 minutes, 2 mL PBS was given as an enema twice for washing, and fluorescence observation was carried out. All images were captured in a dark room. Both white light and fluorescence images were recorded on a hard disk video recorder. S/N ratio was calculated as described previously.²³

2.7 | Immunohistochemistry

Immunohistochemical staining for CEA was carried out using the catalyzed signal amplification (CSA) system, as previously described.²⁶ A rabbit antihuman CEA monoclonal antibody (ab133633; Abcam, Cambridge, UK) was used as the primary antibody. For EGFR staining, the labeled streptavidin-biotin-peroxidase (LSAB) method was carried out as previously described.²⁷ A rabbit antihuman EGFR monoclonal antibody (ab52894; Abcam, Cambridge, UK) was used as the primary antibody.

2.8 | Quantification of CEA-positivity rate in tumor tissues

Carcinoembryonic antigen expression areas were quantified using WinROOF Version 6.3 software (Mitani Corp., Tokyo, Japan) as previously described.²⁸ Briefly, sections were observed and photographed using an Olympus BX50 microscope system (Olympus Corp., Tokyo, Japan). Five randomly selected fields of view (4.3×3.2 mm)

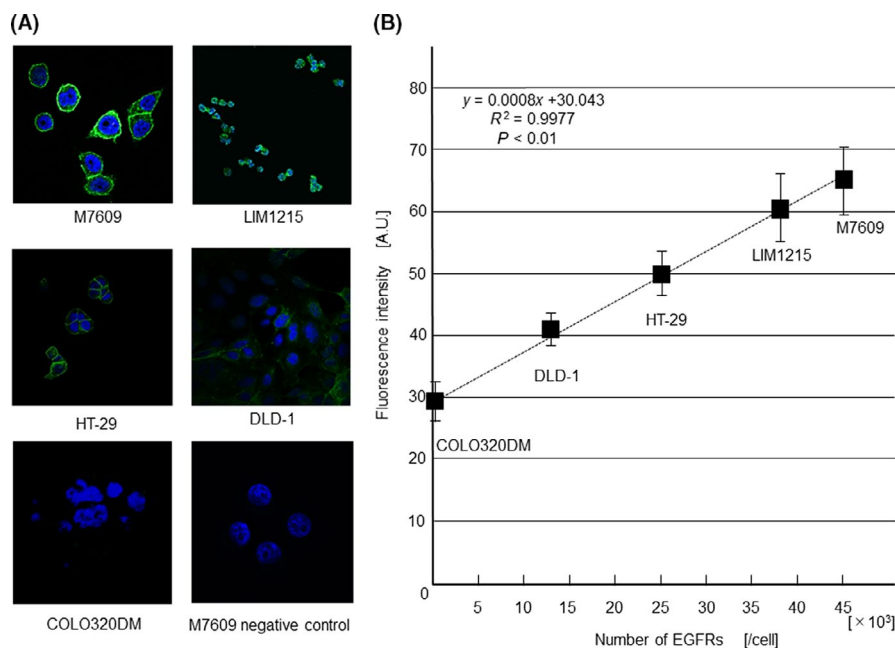


FIGURE 1 Cellular imaging and fluorescence intensity in various colorectal cancer (CRC) cell lines. A, Five CRC cell lines (M7609, LIM1215, HT-29, DLD-1, COLO320DM) were incubated with Alexa Fluor 488-labeled mouse antihuman epidermal growth factor receptor (EGFR) monoclonal antibody (AF488-EGFR-Ab), and then observed by confocal laser microscopy. Alexa Fluor 488-labeled normal mouse IgG2a was used as a negative control. DAPI was used for nuclear staining. B, Fluorescence intensity and number of EGFR in each cell line were determined as described in Materials and Methods². Correlation between fluorescence intensity and number of EGFR was assessed by Pearson's correlation test

were captured at 100 \times magnification, and the CEA expression area that stained brown was extracted automatically using two distinct macroinstructions composed chiefly of algorithms for color extraction based on red-green-blue (RGB) and hue-luminosity-saturation (HLS) parameters. CEA-positive rate was determined by dividing the area stained with diaminobenzidine (DAB) by the entire area selected, and the average rate of the five fields was calculated.

3 | RESULTS

3.1 | Cellular imaging and fluorescence intensity

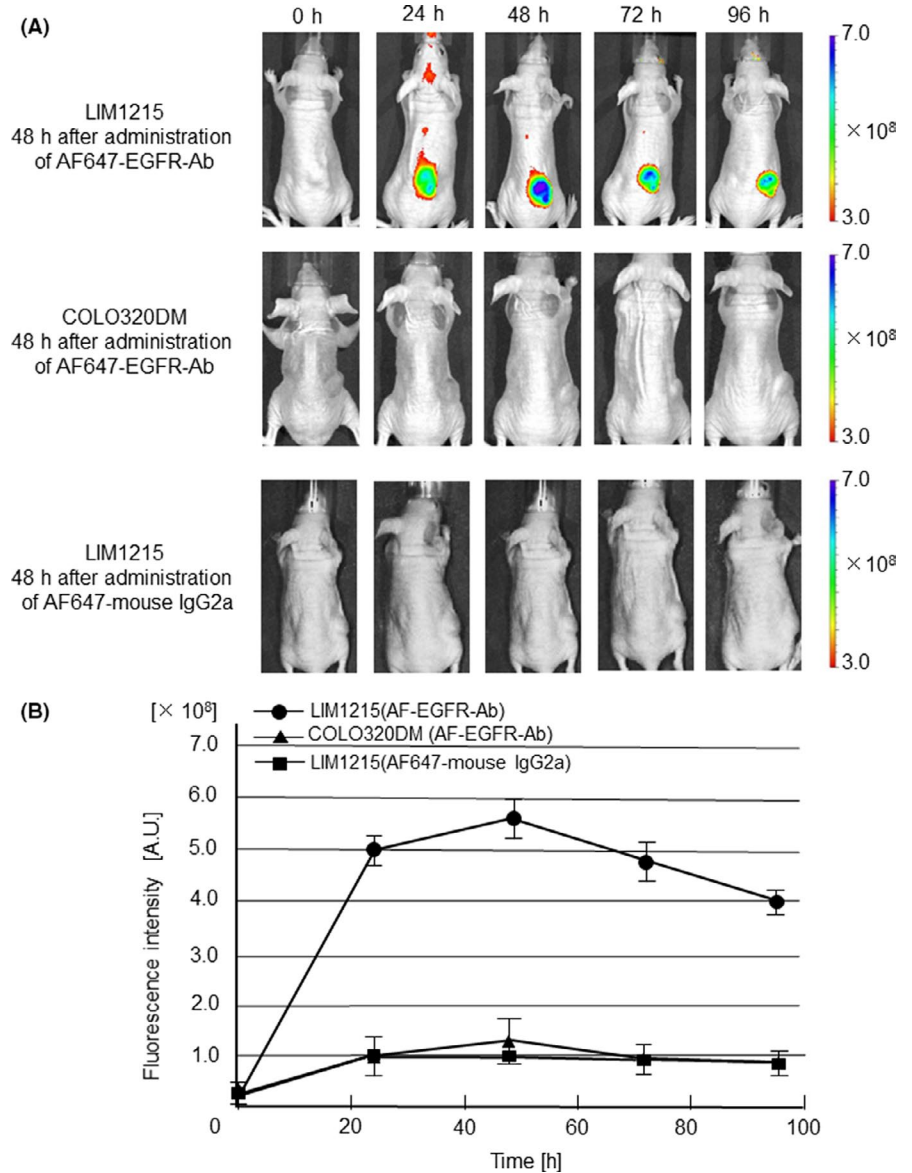
We first attempted to image five CRC cell lines with various expression levels of EGFR using AF488-EGFR-Ab, and determined the fluorescence intensity of each cell line. A strong fluorescent signal was observed along with the cell membrane of M7609 and LIM1215 cells, whereas a medium-intensity fluorescent signal was observed in HT-29 cells (Figure 1A). In contrast, a weak fluorescent signal and almost no signal were observed in DLD-1 and COLO320DM cells, respectively. Almost no signal was observed in M7609 cells treated with AF488-labeled mouse IgG2a as a negative control. The respective fluorescence intensities (mean \pm SD AU/cell) were 65.0 ± 5.6 in M7609, 60.7 ± 5.5 in LIM1215, 50.0 ± 3.6 in HT-29, 41.0 ± 2.7 in DLD-1, and 29.3 ± 3.2 in COLO320DM cells. EGFR expression profile of each cell line was analyzed by flow cytometry (Figure S2). Mean number of EGFR (/cell) was calculated to be 46 100 in M7609, 37 900 in LIM1215,

25 000 in HT-29, 12 800 in DLD-1, and 20 in COLO320DM cells, respectively. There was a significant correlation between fluorescence intensity and the number of EGFR (Figure 1B, $P < .01$ by Pearson's correlation test).

3.2 | In vivo molecular imaging of LIM1215 and COLO320DM xenograft tumors in nude mice

Based on the results of cellular imaging, in vivo molecular imaging was carried out using three mice xenografted with a cell line that highly expresses EGFR (LIM1215) and a low-EGFR expression cell line (COLO320DM). Representative images from each mouse group obtained chronologically are shown in Figure 2A. No fluorescence was observed in the tumor of each mouse before giving AF647-EGFR-Ab. A clear fluorescence signal (5.0×10^8 AU) was observed in the LIM1215 cell tumor at 24 hours. The fluorescence intensity reached a maximum (5.6×10^8 AU) at 48 hours, and then gradually decreased until 96 hours. In contrast, in the COLO320DM cell tumor, almost no fluorescence signal was observed at any time. When AF647-labeled mouse IgG2a was given to mice as negative control, no significant signals were observed at any timepoint. The remaining two mice with LIM1215 and COLO320DM cell tumors given with AF647-EGFR-Ab showed similar imaging patterns. The mean fluorescence intensity from three mice at each timepoint is shown in Figure 2B. There were significant differences in fluorescence intensities between the LIM1215 and COLO320DM cell tumor groups at all timepoints from 24 to 96 hours ($P < .01$ by Student's *t* test).

FIGURE 2 Chronological changes of in vivo molecular imaging of LIM1215 and COLO320DM xenograft tumors in nude mice. A, Nude mice xenografted with LIM1215 or COLO320DM cells were injected with AF647-epidermal growth factor receptor (EGFR)-Ab into the tail vein, and tumors were observed using an IVIS Spectrum system (Perkin Elmer, Waltham, MA, USA). Alexa Fluor 647-labeled normal mouse IgG2a was used as a negative control. B, Mean fluorescence intensity of the tumors from three mice (\pm SD) at each timepoint is shown



3.3 | In vivo molecular imaging of LIM1215 xenograft tumors treated with 5-FU

We next evaluated fluorescence images of LIM1215 xenograft tumors in five nude mice treated with 5-FU and compared them with those of five mice treated with vehicle alone, according to the treatment schedule described in Figure S1a. Figure 3A shows representative images of the tumors in mice treated with vehicle alone or 5-FU at 48 hours after giving AF647-EGFR-Ab. A clear fluorescent signal was detected in the site of the tumor of the control mouse (5.4×10^8 AU), whereas a weaker fluorescent signal was detected in the site of the tumor of the treated mouse (3.8×10^8 AU). The remaining four mice treated with 5-FU or vehicle alone showed similar patterns. The mean fluorescence intensity (\pm SD) of the tumor in each mouse over time was plotted after giving AF647-EGFR-Ab (Figure 3B). Fluorescence intensity abruptly increased at 24 hours, reaching a maximum at 48 hours, and then gradually decreased

until 120 hours in both the treatment group and the control group. However, the mean fluorescence intensities in the treatment group were significantly lower than those in the control group at all timepoints from 24 to 120 hours ($P < .01$ by Student's *t* test). Similar results were obtained using another CRC cell line PMF-ko14 as a xenograft tumor (Figure S3). These data clearly indicate that treatment with anticancer drugs reduced the number of EGFR-expressing tumor cells.

To investigate whether our EGFR imaging method is able to precisely evaluate the therapeutic efficacy of anticancer drugs, we quantified fluorescence intensity and determined its correlation with viable cell volume in LIM1215 xenograft tumors in mice before and after treatment with 5-FU. Figure 4A shows changes in tumor volumes measured using Vernier calipers before and 3 weeks after the start of treatment. Despite giving 5-FU, the volumes of six tumors increased after treatment as compared with the volume before treatment, whereas the volume of two tumors showed almost

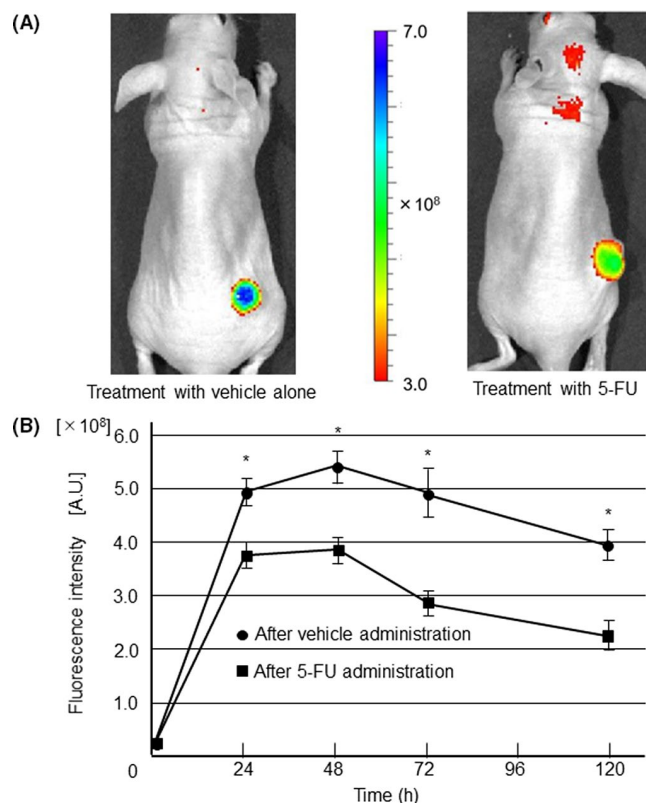


FIGURE 3 In vivo molecular imaging of LIM1215 xenograft tumor treated with fluorouracil (5-FU). A, Mice were i.p. treated three times with 5-FU or vehicle alone as described in Figure S1a, and then injected with AF647-epidermal growth factor receptor (EGFR)-Ab, after which fluorescence imaging was done using an IVIS Spectrum system (Perkin Elmer, Waltham, MA, USA). Representative images of tumors in mice treated with vehicle alone or 5-FU 48 h after giving AF647-EGFR-Ab are shown. B, Mean fluorescence intensity (\pm SD) of the tumors observed in five mice at each timepoint is shown. * $P < .01$ by Student's *t* test

no change after treatment. However, the fluorescence intensities in all eight tumors decreased after treatment (Figure 4B). To evaluate cell viability in tumors histologically, we excised the tumors and carried out H&E staining. Representative H&E staining patterns in tumors after treatment with 5-FU and vehicle alone are shown in Figure 4C,D. H&E staining of tumors treated with vehicle alone showed compacted viable tumor cells without a fibrotic and necrotic pattern (Figure 4C). In contrast, H&E staining in 5-FU-treated tumor tissue showed extensive fibrosis and necrosis (Figure 4D).

In order to quantify the viable cells in tumor tissues, we carried out immunohistochemical staining for CEA, which is reportedly a good marker of CRC cells with high sensitivity and specificity.^{29,30} Representative CEA staining patterns in tumors after treatment with vehicle alone or 5-FU are shown in Figure 4E,F. Immunostaining of tumors treated with vehicle alone for CEA showed that most of the cells were positive for CEA (Figure 4E). In contrast, immunostaining for CEA in 5-FU-treated tumor tissue showed a reduced number of positive cells resulting in a dappled distribution of signals (Figure 4F). The mean CEA-positivity rate in 5-FU-treated tumors

was $31.4 \pm 11.1\%$, which was significantly lower than that in the control group treated with vehicle alone ($72.6 \pm 3.0\%$, Figure 4G). Moreover, there was a significant correlation between the percentage decrease in fluorescence intensity and the CEA-positivity rate in each tumor (Figure 4H, $P < .01$ by Pearson's correlation test). These data suggest that fluorescence intensity reflects the viable cell volume of the tumor after treatment with anticancer drugs. Thus, our imaging method is suitable for evaluation of the therapeutic efficacy of anticancer drugs.

3.4 | Molecular imaging of colorectal tumors by endoscopy in AOM-treated rats

In vivo molecular imaging of colorectal tumors in AOM-treated rats was carried out using a veterinary endoscope. Representative images of a tumor under white light and EGFR fluorescent imaging (rats #1, #3) are shown in Figure 5A-D. A flat isochromatic tumor was observed in the colorectum under white light. When the fluorescent probe was administered by enema into the colorectum (rectum to splenic flexure) followed by washing with PBS, a strong green fluorescence signal was observed at the same site in the rectum. Mean S/N ratio calculated from fluorescent intensities of all polyps was 10.6 ± 0.7 (Figure S4). When the colorectum was pretreated with non-labeled anti-EGFR antibody, the fluorescent signal was significantly suppressed (Figure 5C,D), suggesting specificity of EGFR-targeted imaging with anti-EGFR-Ab. The S/N ratio also significantly decreased (1.6 ± 0.4 , $P < .01$ by Student's *t* test; Figure S4).

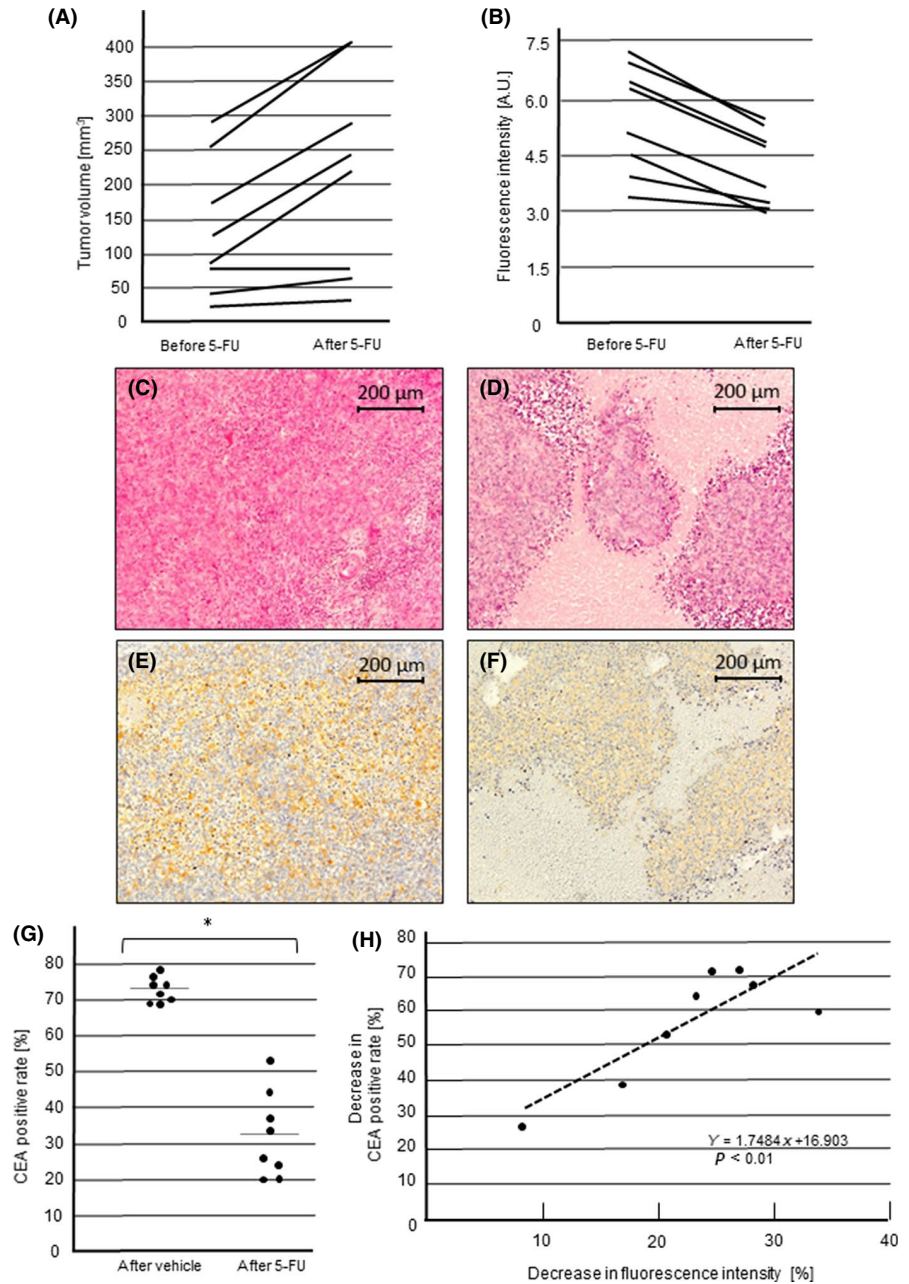
Observation of the colorectal mucosa removed from the mouse showed a polyp that was visible to the naked eye (Figure 5E). The tumor was diagnosed as adenoma based on histological staining with H&E staining (Figure 5F). EGFR immunohistochemistry of the lesion showed a clear expression of EGFR in the tumor cells (Figure 5G) despite a faint non-specific signal with rabbit IgG as a negative control (Figure 5H).

We observed colorectums of 10 rats using white light and fluorescence imaging with AF488-EGFR-Ab. White light observation showed one polyp in each colorectum of six rats, and no polyps in the colorectum of the remaining four rats. Average diameter of the polyps observed was 2.17 ± 0.37 mm. Molecular imaging with AF488-EGFR-Ab detected all these polyps in the same location as that observed with white light, although no additional new polyps were detected (Table 1). These results suggest that EGFR molecular imaging using our veterinary fluorescent endoscopic system may be able to detect a small polyp with a diameter of approximately 2 mm.

4 | DISCUSSION

In the present study, we clearly visualized CRC cells using non-invasive optical molecular imaging with a fluorescence-conjugated anti-EGFR antibody in vitro and in vivo in correlation with the degree of EGFR expression. Moreover, we showed that EGFR fluorescence intensity accurately reflected the viable cell volume in tumors after

FIGURE 4 Relationship between epidermal growth factor receptor (EGFR) fluorescence intensity and tumor viability with or without fluorouracil (5-FU) treatment. A, Tumor volumes of xenografts in each mouse ($n = 8$) before and after 5-FU treatment were plotted. B, Fluorescence intensity of the xenograft tumor before and after 5-FU treatment in each mouse was plotted. C-F, Representative H&E and carcinoembryonic antigen (CEA) staining patterns in the tumor after vehicle alone or 5-FU treatment. H&E staining after vehicle treatment (C), or 5-FU treatment (D), immunohistochemical staining for CEA after vehicle treatment (E), or 5-FU treatment (F) is shown. G, CEA-positive rates in the tumor after vehicle treatment and 5-FU treatment were plotted. $*P < .01$ by Student's *t* test. H, Correlation between the percentage decrease of the CEA-positive rate and percentage decrease of fluorescence intensity in each tumor was assessed by Pearson's correlation test



treatment with 5-FU. This is essentially the first study to show the possibility that molecular imaging of EGFR is useful for evaluating the effect of chemotherapy. Although we evaluated the therapeutic efficacy of 5-FU using a xenograft model rather than an orthotopic colorectal tumor model, our results may suggest that EGFR molecular imaging is useful for evaluation of CRC primary lesions using fluorescence endoscopy. Furthermore, we were able to detect a benign small adenoma in the rat colorectum using anti-EGFR fluorescence imaging. This molecular imaging method may lead to the development of a new endoscopic detection method with less oversight for the detection of small benign tumors as well as for malignant tumors.

Previous studies have used molecular imaging for adenoma and adenocarcinoma using various fluorescent probes such as protease-activatable fluorescent probe,³¹

γ -glutamyltranspeptidase-activatable probe,³² and fluorescent-labeled AKPGYLS peptide multimer.³³ Because anti-EGFR antibodies such as cetuximab and panitumumab are currently used worldwide in clinical practice for the treatment of CRC,^{34,35} it would be relatively easy to apply fluorescent-labeled anti-EGFR antibody for the diagnosis of human tumors. Moreover, when AF-EGFR-Ab was given i.v. in mice, it showed specific and strong binding to EGFR in the xenograft tumor model continuously for up to approximately 96 hours after dosage, indicating advantages for future clinical application. However, because AF-EGFR-Ab used in the xenograft experiments showed very little reactivity to mouse EGFR (Figure S5), further experiments including fluorescent intensity in tumor and background (S/N ratio) with a syngeneic mouse model are required.

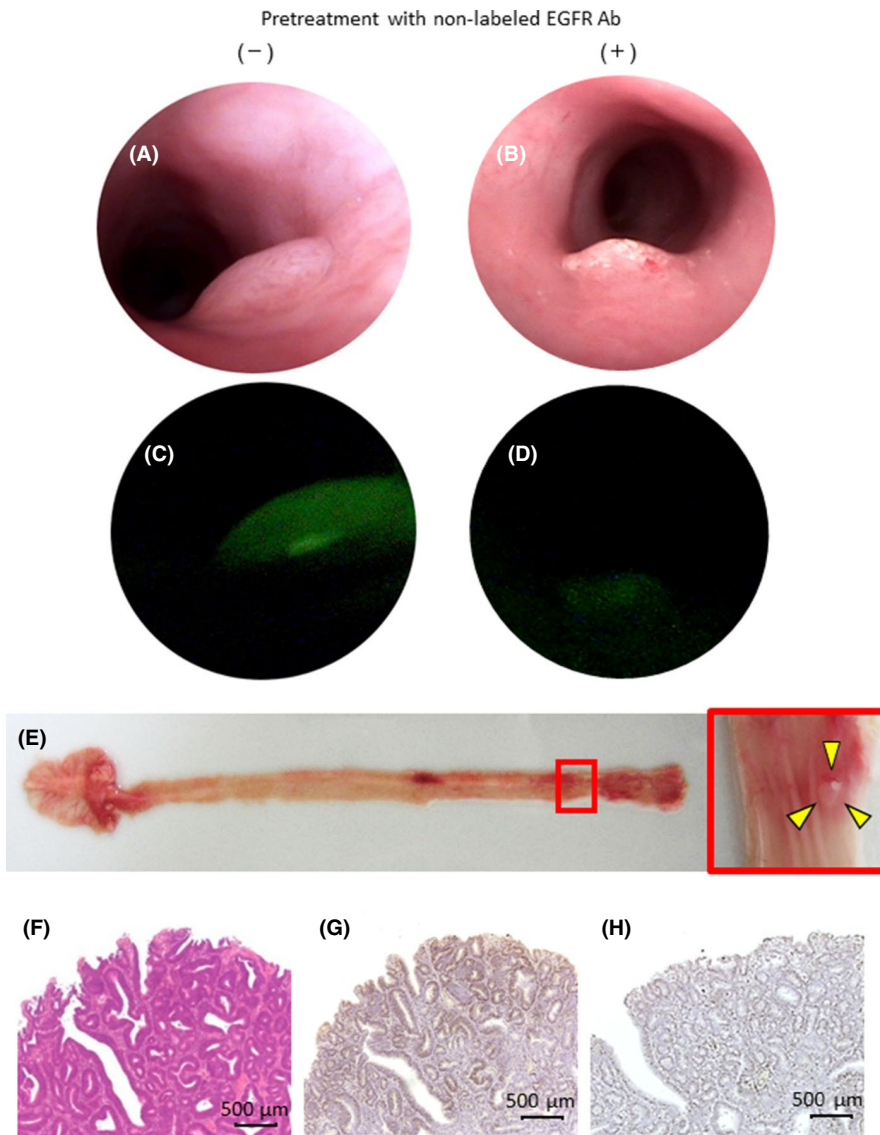


FIGURE 5 Endoscopic and histological findings of colorectal polyps from azoxymethane (AOM)-treated rats. A,B, Representative endoscopic image of a colorectal polyp in an AOM-injected rat (rats #1, #3) observed using a thin endoscope. C,D, A 3-mL aliquot of AF488-epidermal growth factor receptor (EGFR)-Ab (20 $\mu\text{g}/\text{mL}$) was given by enema with or without pretreatment with non-labeled EGFR-Ab (200 $\mu\text{g}/\text{mL}$), and colorectal polyps were detected by fluorescent thin endoscopy. E, The entire colorectum was removed from the rat. Yellow arrows show a small polyp. F, Histopathological findings of the resected tumor (H&E). G, EGFR immunohistochemical staining of the polyp. H, Treatment with normal rabbit IgG as a negative control

Currently, clinical evaluation of the therapeutic effect of anti-cancer agents on solid cancers is done using RECIST guidelines.^{6,7} RECIST assessment is carried out by measuring the diameter of each tumor before and after treatment using CT images. However, often the tumor size in a CT image does not reflect viable tumor cell volume. In this respect, the method to detect only viable cells in the tumor is superior to the RECIST method with CT images for evaluating therapeutic efficacy. For example, positron-emission tomography (PET) imaging with fluorodeoxyglucose (FDG) probes has become a valuable method for clinicians because it reflects tumor viability of primary CRC and/or metastatic tumors. Recently, Turker and associates synthesized a novel PET imaging probe conjugated with a Fab' fragment of an anti-EGFR antibody and showed that it detected colitis-associated cancer in mice with a high target-to-background ratio.³⁶ However, given the longer survival period of CRC patients as a result of the use of molecular-targeting agents, it is not practical to repeatedly use this radioactive modality in patients.^{37,38} Optical molecular imaging technologies, such as the one used in the present study, are less harmful and easier to use than procedures

TABLE 1 Colorectal polyps detected by white light and EGFR molecular imaging using an animal endoscope in an AOM-treated rat model

Rat no.	White light image (n)	EGFR molecular image (n)	Size (mm)
1	1	1	3
2	0	0	0
3	1	1	2
4	1	1	2
5	0	0	0
6	1	1	2
7	0	0	0
8	1	1	2
9	0	0	0
10	1	1	2
Total	6	6	

AOM, azoxymethane; EGFR, epidermal growth factor receptor.

involving radioactive agents. Here, we showed that our EGFR-targeted imaging reflected viable tumor cells. This was also consistent with our *ex vivo* data of xenograft tumors in terms of distribution of AF-EGFR-Ab; when frozen sections of tumor were observed at low magnification under fluorescent microscopy, strong fluorescent signals were detected throughout the tumor from mice treated with vehicle alone, whereas reduced levels of fluorescence were detected in tumors from mice treated with 5-FU that gave a dappled distribution of signals (Figure S6). However, the relationship between fluorescent intensity and viable tumor cell volume should be investigated further. In addition, our EGFR-targeted imaging to evaluate the effects of cancer therapy assumes that EGFR expression is not downregulated or upregulated by the chemotherapy itself. To address this point, we investigated relative mRNA levels and EGFR number in CRC cells before and after 5-FU treatment, and confirmed that there are no significant changes before and after 5-FU treatment (Figure S7). Thus, EGFR-targeted imaging is a potentially useful tool for evaluating therapeutic efficacy.

In the present study, we were able to detect all six small adenomas that were 2–3 mm in diameter. To date, no studies have reported the detection of colorectal adenomas using EGFR-targeted molecular imaging. Thus, EGFR-targeted molecular imaging may lead to the development of a sensitive detection method for adenoma. However, this study was limited to cell lines and animal experiments and, therefore, further investigation for clinical application will be needed.

For clinical administration with fluorescent probes, two routes can be used to give AF-EGFR-Ab: local administration by direct spraying and *i.v.* administration. In the present study, we gave AF-EGFR-Ab by enema and obtained a relatively high S/N ratio (10.6 ± 0.7). When AF-EGFR-Ab was given *i.v.* to mice in preliminary experiments, the tumor was also visualized with the fluorescent signal although the S/N ratio was relatively low (4.0 ± 0.6 ; Figure S8). Further experiments with more animals are required to compare the two administration routes.

Image brightness of the veterinary endoscope used in this study was low as a result of its thinness (Figure 5A), and the brightness of our fluorescence endoscopy system with the blue and yellow filters was much lower (Figure 5B). Brightness of the thin endoscope and the fluorescence endoscope with the two filters was calculated to be 23.7 and 4.8 lumens, respectively, based on the illumination intensities (data not shown). However, the image brightness of endoscopes for use in humans is now up to approximately 800 lumens (unpublished data, Olympus Corp., 2017). The brightness of the autofluorescence endoscope (AFI; Olympus Corp.) is approximately half that value, which is approximately 100-fold higher as compared with the veterinary fluorescent endoscope used in the present study. Therefore, when fluorescence molecular imaging of EGFR is applied to future human colonoscopy, it will be possible to obtain much brighter and clearer images for detection of colorectal tumors.

In conclusion, the results of our animal experiments suggest that EGFR-targeted molecular imaging may be useful for evaluating chemotherapeutic efficacy, as indicated by viable cell volume, more

accurately than tumor size. This EGFR imaging method may also be useful in detecting colorectal adenoma in the colorectum for colonoscopy. This imaging method may lead to advancements in early detection and improved diagnosis of colorectal tumors, as well as therapeutic evaluation of CRC.

ACKNOWLEDGMENTS

The authors are grateful to Dr Masayuki Shono and Dr Kazuki Horikawa for their expert technical assistance.

DISCLOSURE

Authors declare no conflicts of interest for this article.

ORCID

Yoshihiko Miyamoto  <https://orcid.org/0000-0002-4876-9156>

Tetsuji Takayama  <https://orcid.org/0000-0002-0175-1573>

REFERENCES

1. Torre LA, Siegel RL, Ward EM, et al. Global cancer incidence and mortality rates and trends—an update. *Cancer Epidemiol Biomarkers Prev.* 2016;25:16–27.
2. Fearon ER, Vogelstein B. A genetic model for colorectal tumorigenesis. *Cell.* 1990;61:759–767.
3. Kinzler KW, Vogelstein B. Lessons from hereditary colorectal cancer. *Cell.* 1996;87:159–170.
4. Leslie A, Carey FA, Pratt NR, et al. The colorectal adenoma-carcinoma sequence. *Br J Surg.* 2002;89:845–860.
5. van Rijn JC, Reitsma JB, Stoker J, et al. Polyp miss rate determined by tandem colonoscopy: a systematic review. *Am J Gastroenterol.* 2006;101:343–350.
6. Trillet-Lenoir V, Freyer G, Kaemmerlen P, et al. Assessment of tumour response to chemotherapy for metastatic colorectal cancer: accuracy of the RECIST criteria. *Br J Radiol.* 2002;75:903–908.
7. Eisenhauer EA, Therasse P, Bogaerts J, et al. New response evaluation criteria in solid tumours: revised RECIST guideline (version 1.1). *Eur J Cancer.* 2009;45:228–247.
8. Richards CH, Roxburgh CS, Anderson JH, et al. Prognostic value of tumour necrosis and host inflammatory responses in colorectal cancer. *Br J Surg.* 2012;99:287–294.
9. Pollheimer MJ, Kornprat P, Lindtner RA, et al. Tumor necrosis is a new promising prognostic factor in colorectal cancer. *Hum Pathol.* 2010;41:1749–1757.
10. Komori K, Kanemitsu Y, Kimura K, et al. Tumor necrosis in patients with TNM stage IV colorectal cancer without residual disease (R0 Status) is associated with a poor prognosis. *Anticancer Res.* 2013;33:1099–1105.
11. Weissleder R. Molecular imaging in cancer. *Science.* 2006;312:1168–1171.
12. Mahmood U, Wallace MB. Molecular imaging in gastrointestinal disease. *Gastroenterology.* 2007;132:11–14.
13. Normanno N, De Luca A, Bianco C, et al. Epidermal growth factor receptor (EGFR) signaling in cancer. *Gene.* 2006;366:2–16.
14. Abd El All HS, Mishriky AM, Mohamed FA. Epidermal growth factor receptor in colorectal carcinoma: correlation with clinico-pathological prognostic factors. *Colorectal Dis.* 2008;10:170–178.

15. Galizia G, Lieto E, Orditura M, et al. Epidermal growth factor receptor (EGFR) expression is associated with a worse prognosis in gastric cancer patients undergoing curative surgery. *World J Surg.* 2007;31:1458-1468.
16. Spano JP, Lagorce C, Atlan D, et al. Impact of EGFR expression on colorectal cancer patient prognosis and survival. *Ann Oncol.* 2005;16:102-108.
17. Cohen G, Lecht S, Arien-Zakay H, et al. Bio-imaging of colorectal cancer models using near infrared labeled epidermal growth factor. *PLoS ONE.* 2012;7:e48803.
18. Cohen G, Lecht S, Oron-Herman M, et al. Near infrared optical visualization of epidermal growth factor receptors levels in COLO205 colorectal cell line, orthotopic tumor in mice and human biopsies. *Int J Mol Cell.* 2013;14:14669-14688.
19. Goetz M, Ziebart A, Foersch S, et al. In vivo molecular imaging of colorectal cancer with confocal endomicroscopy by targeting epidermal growth factor receptor. *Gastroenterology.* 2010;138:435-446.
20. Goetz M, Hoetker MS, Diken M, et al. In vivo molecular imaging with cetuximab, an anti-EGFR antibody, for prediction of response in xenograft models of human colorectal cancer. *Endoscopy.* 2013;45:469-477.
21. Liu J, Zuo X, Li C, et al. In vivo molecular imaging of epidermal growth factor receptor in patients with colorectal neoplasia using confocal laser endomicroscopy. *Cancer Lett.* 2013;330:200-207.
22. Okada Y, Kimura T, Nakagawa T, et al. EGFR downregulation after anti-EGFR therapy predicts the antitumor effect in colorectal cancer. *Mol Cancer Res.* 2017;15:1445-1454.
23. Fujimoto S, Muguruma N, Okamoto K, et al. A novel theranostic combination of near-infrared fluorescence imaging and laser irradiation targeting c-KIT for gastrointestinal stromal tumors. *Theranostics.* 2018;8:2313-2328.
24. Tomayko MM, Reynolds CP. Determination of subcutaneous tumor size in athymic (nude) mice. *Cancer Chemother Pharmacol.* 1989;24:148-154.
25. Euhus DM, Hudd C, LaRegina MC, et al. Tumor measurement in the nude mouse. *J Surg Oncol.* 1986;31:229-234.
26. Mizuki H, Kawamura T, Nagasawa D. In situ immunohistochemical detection of intracellular *Mycoplasma salivarium* in the epithelial cells of oral leukoplakia. *J Oral Pathol Med.* 2015;44:134-144.
27. Inoue A, Okamoto K, Fujino Y, et al. B-RAF mutation and accumulated gene methylation in aberrant crypt foci (ACF), sessile serrated adenoma/polyp (SSA/P) and cancer in SSA/P. *Br J Cancer.* 2015;112:403-412.
28. Hatanaka Y, Hashizume K, Nitta K, et al. Cytometrical image analysis for immunohistochemical hormone receptor status in breast carcinomas. *Pathol Int.* 2003;53:693-699.
29. Tiernan JP, Perry SL, Verghese ET, et al. Carcinoembryonic antigen is the preferred biomarker for in vivo colorectal cancer targeting. *Br J Cancer.* 2013;108:662-667.
30. Davidson BR, Sams VR, Styles J, et al. Comparative study of carcinoembryonic antigen and epithelial membrane antigen expression in normal colon, adenomas and adenocarcinomas of the colon and rectum. *Gut.* 1989;30:1260-1265.
31. Funovics MA, Alencar H, Montet X, et al. Simultaneous fluorescence imaging of protease expression and vascularity during murine colonoscopy for colonic lesion characterization. *Gastrointest Endosc.* 2006;64:589-597.
32. Mitsunaga M, Kosaka N, Choyke PL, et al. Fluorescence endoscopic detection of murine colitis-associated colon cancer by topically applied enzymatically rapid-activatable probe. *Gut.* 2013;62:1179-1186.
33. Joshi BP, Liu Z, Elahi SF, et al. Near-infrared-labeled peptide multimer functions as phage mimic for high affinity, specific targeting of colonic adenomas in vivo (with videos). *Gastrointest Endosc.* 2012;76:1197-1206.e1-5.
34. Cunningham D, Humblet Y, Siena S, et al. Cetuximab monotherapy and cetuximab plus irinotecan in irinotecan-refractory metastatic colorectal cancer. *N Engl J Med.* 2004;351:337-345.
35. Garrett CR, Bekaii-Saab TS, Ryan T, et al. Randomized phase 2 study of pegylated SN-38 (EZN-2208) or irinotecan plus cetuximab in patients with advanced colorectal cancer. *Cancer.* 2013;119:4223-4230.
36. Turker NS, Heidari P, Kucherlapati R, et al. An EGFR targeted PET imaging probe for the detection of colonic adenocarcinomas in the setting of colitis. *Theranostics.* 2014;4:893-903.
37. Yamada Y, Takahari D, Matsumoto H, et al. Leucovorin, fluorouracil, and oxaliplatin plus bevacizumab versus S-1 and oxaliplatin plus bevacizumab in patients with metastatic colorectal cancer (SOFT): an open-label, non-inferiority, randomised phase 3 trial. *Lancet Oncol.* 2013;14:1278-1286.
38. Baba H, Yamada Y, Takahari D, et al. S-1 and oxaliplatin (SOX) plus bevacizumab versus mFOLFOX6 plus bevacizumab as first-line treatment for patients with metastatic colorectal cancer: updated overall survival analyses of the open-label, non-inferiority, randomised phase III: SOFT study. *ESMO Open.* 2017;2:e000135.

SUPPORTING INFORMATION

Additional supporting information may be found online in the Supporting Information section at the end of the article.

How to cite this article: Miyamoto Y, Muguruma N, Fujimoto S, et al. Epidermal growth factor receptor-targeted molecular imaging of colorectal tumors: Detection and treatment evaluation of tumors in animal models. *Cancer Sci.* 2019;110:1921-1930. <https://doi.org/10.1111/cas.14020>